Journal of Power Sources 273 (2015) 1142–1147

Contents lists available at ScienceDirect

Journal of Power Sources

journal homepage: www.elsevier.com/locate/jpowsour

Catalytic behavior of a palladium doped binder free paper based cobalt electrode in electroreduction of hydrogen peroxide

Dongming Zhang, Ke Ye, Dianxue Cao, Jinling Yin, Kui Cheng, Bin Wang, Yang Xu, Guiling Wang*

Key Laboratory of Superlight Materials and Surface Technology of Ministry of Education, College of Materials Science and Chemical Engineering, Harbin Engineering University, Harbin 150001, PR China

HIGHLIGHTS

- A binder free PG-CoPd electrode is employed for H_2O_2 electroreduction.
- The Co exhibits a 3D nano-plates structure on the 1D paper surface.
- The PG-CoPd exhibits high catalytic activity and stability during the whole test.

GRAPHICAL ABSTRACT

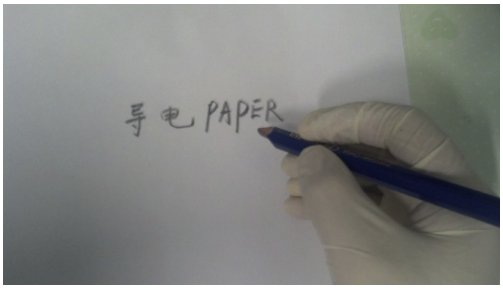

ARTICLE INFO

Article history:
Received 26 June 2014
Received in revised form
12 September 2014
Accepted 2 October 2014
Available online 13 October 2014

Keywords:
Flexible
Nano-plate
Binder free
Hydrogen peroxide electroreduction

ABSTRACT

A piece of flexible and conductive A4 paper is prepared by coating a layer of graphite with a normal 8B pencil. Then, Co nano-plates and Pd are assembled by a simple electrodeposition and chemical-reduction methods on the surface of the electrified paper, respectively. The as-prepared paper substrate/graphite-Co film-Pd (PG-CoPd) electrode is characterized by scanning electron microscopy equipped with energy dispersive X-ray spectrometer, transmission electron microscope and X-ray diffractometer. The catalytic activity of the PG-CoPd electrode for H_2O_2 electroreduction is investigated by means of cyclic voltammetry and chronoamperometry. The preparation process of the PG-CoPd electrode does not use any binder and it exhibits a three dimensional (3D) nano structure, high stability and good electric conductivity. The mass of the Pd in PG-CoPd is about 0.0535 mg cm^{-2} and the reduction current density reaches to −4.30 A cm^{-2} mg^{-1} in 1 mol dm^{-3} NaOH and 1.4 mol dm^{-3} H_2O_2 at −0.5 V, which is higher than our previous reports of Au/Pd modified Co electrode.

© 2014 Elsevier B.V. All rights reserved.

1. Introduction

Hydrogen peroxide (H_2O_2) has been regarded as a promising oxidizer for liquid-based fuel cells (FCs), such as metal semi-fuel cells (MSFCs) [1–3], direct borohydride fuel cells (DBFCs) [4–6], direct methanol fuel cells (DMFCs) [7–9], direct peroxide fuel cells (DPFCs) [10–14]. Compared to oxygen, the electroreduction of H_2O_2 takes place via a two-electron transfer involving the breakage of single dioxygen bonds rather than the breakage of double bonds for O_2 reduction [15,16]. So, its electroreduction has a lower activation barrier and faster kinetics than O_2. Besides, H_2O_2 is in liquid form, which is easier for the fuel cells design, assembly and operation. These FCs employing H_2O_2 as oxidizer were developed as underwater or space power sources working in air-free environments [1,4].

The cathode performance is one of a key factor that decides the application of the FCs and the electrode material has a great impact on

* Corresponding author. Tel./fax: +86 451 82589036.
E-mail address: wangguiling@hrbeu.edu.cn (G. Wang).

http://dx.doi.org/10.1016/j.jpowsour.2014.10.014
0378-7753/© 2014 Elsevier B.V. All rights reserved.

the electrochemical reaction rate of the H_2O_2 electroreduction. So the study of electrode material for the H_2O_2 electroreduction has become a hot topic in recent years. Precious metals (Eg. Pd, Au, Ag) have a high catalytic activity for the H_2O_2 electroreduction [17–20]. However, their extensive utilization is restricted by the high cost. Nowadays, transition metals and their oxides (Eg. Co, Co_3O_4, Fe_2O_3) [18,20,21] have been investigated as low cost catalysts for H_2O_2 electroreduction. Compared with metal oxides, the metallic metals have higher electronic conductivity. Unfortunately, their electrocatalytic activities are much lower than the precious metals. So, the combination of precious metals and non-precious metals has become an interesting work [18,20]. Recently, our group prepared Au and Pd modified porous Co electrodes for H_2O_2 electroreduction and their reduction current densities reached to −2.10 and −4.00 A cm^{-2} mg^{-1}, respectively, at −0.5 V in 1.5 mol dm^{-3} H_2O_2 [18].

Traditionally, carbon materials based metal catalysts electrodes have been widely used in FCs and such electrodes are employed with success since more than a decade [6,9,22]. However, most of carbon based electrode materials must employ expensive binder to ensure them coating on the surface of the collectors [6,9,21,22]. Besides, the existence of the binder may reduce the electric conductivity of the electrode and may fall off from the collectors during the long test process, both of which will cut down the electrochemical catalytic activity of the work electrode. Nowadays, electrodeposition method [5,19,20] has developed as a facile way to prepare stable electrodes without binder and slurry-coating process.

Metal materials are the most widely used substrates for the assembling of the electrodes [10,14,17,18,22]. However, the metal resources are limited and they are easy to be etched in the alkaline or acerbic environment. Besides, the shapes of the metals materials are unalterable and easy to be damaged.

Nowadays, flexible and non-metallic electrode substrates (Eg. carbon paper, carbon cloth, sponge, textile) [11–13,23–27] have become a research hotspot. Cui et al. fabricated flexible sponge-carbon nanotube (CNT) supported Pt electrode for microbial fuel cells [23] and assembled deformable textile-graphene supported MnO_2 for electrochemical capacitors [24]. Our team fabricated Ni@multi-walled carbon nanotubes (MWNTs)/Sponge [26] and Ni@MWNTs/Fabric [27] electrodes for the electrooxidation of $NaBH_4$ and H_2O_2. Both of the sponge and textile exhibit good stability and high electrochemical performance in test solutions. However, the preparation technologies of the carbon nanotubes and graphene are complicated and the costs are somewhat high.

The paper, one of the great inventions of people, is produced easily and disposable, and has been researched in laboratories for e-applications [28–32]. Cui et al. [29] reported a kind of lithium battery employed Ag modified paper as the electrode substrate. Chan et al. [30] fabricated full cells employing $Li_4Ti_5O_{12}$ and $LiCoO_2$ powders deposited onto current collectors consisting of paper coated with carbon nanotubes. In the same box, the high cost of Ag ink and CNTs may restrict their extensive utilization.

In this paper, a layer of graphite is coated on the surface of a piece of A4 paper to act as a flexible current collector and Co nano-plates are electrodeposited on the A4-8B substrate. In order to obtain a higher catalytic activity, metallic Pd is prepared by a facile chemical-reduction method. The paper substrate/graphite-Co film-Pd (PG-CoPd) electrode exhibits a special three dimensional (3D) nano structure. Besides, the PG-CoPd electrode provides a high electrocatalytic activity and superior stability for the electroreduction of H_2O_2.

2. Experimental

All chemicals were analytical grade and were used without further purification. The A4 paper (70 g m^{-2}, Shenyang Jinxin office equipment Co. Ltd.) is commercially available printing paper. The fabrication process of the paper substrate/graphite-Co film-Pd (PG-CoPd) electrode is shown in Fig. 1. First, a common 8B pencil (Shanghai Yinzun company) was used to draw on the A4 paper uniformly and form a conductive paper substrate/graphite (PG) current collector. The mass of the graphite layer in the electrode is 0.6 mg cm^{-2} and the sheet resistance is about 20 Ω/square. Second, the as-prepared PG collector was cut into 1 × 1 cm^2 and then immersed in 2.5 mol dm^{-3} KCl, 0.4 mol dm^{-3} NH_4Cl, 0.5 mol dm^{-3} H_3BO_3 and 1.0 mol dm^{-3} $CoCl_2 \cdot 6H_2O$ for the electrodeposition of Co nano-plates on the PG substrate, which was performed using the Autolab PGSTAT302 (Eco Chemie) electrochemical workstation in a conventional three electrode electrochemical cell with a saturated Ag/AgCl, KCl reference electrode and Pt foil counter electrode. First was a 20 min 1.0 V oxidation potential which made the graphite surface transform into a hydrophilic surface. Then the electrodeposition was carried out at a constant potential of −0.8 V for 150 min to form the PG-Co. The mass of the Co nanoplates on the electrode is about 8 mg cm^{-2}. At last, the PG-CoPd electrode was prepared by immersing the as-prepared PG-Co into a solution containing 1 mmol dm^{-3} $PdCl_2$ solution for 30 s (Eq. (1)).

$$Co + Pd^{2+} \rightarrow Co^{2+} + Pd \quad (1)$$

H_2O_2 electroreduction was also performed in the same three-electrode electrochemical cell using the 1 cm^2 PG-CoPd electrode. All potentials were referred to the saturated Ag/AgCl, KCl reference electrode. The morphology of the electrodes was determined using a scanning electron microscope equipped with energy dispersive X-ray spectrometer (SEM, JEOL JSM-6480) and transmission electron microscope (TEM, FEI TeccaiG2S-Twin, Philips). The structure was analyzed by a powder X-ray diffractometer (XRD, Rigaku TTR-III) equipped with Co Kα radiation ($\lambda = 0.17889$ nm). The Pd loading was measured using an inductive coupled plasma emission spectrometer (ICP, Xseries II, Thermo Scientific). The catalysts that employed for the TEM characterization are prepared as follows: the Co and CoPd nano-plates were scraped off from the as-prepared PG-Co and PG-CoPd electrodes and then dispersed into 10 mL ethanol by ultrasonication, following by dropping 50 μL of the suspension onto the lacey support film and dried in air.

3. Results and discussion

Fig. 2 shows the SEM images of the PG (Fig. 2a and b), PG-Co (Fig. 2c and d), PG-CoPd electrode (Fig. 2e and f) and TEM images of the Co (Fig. 2g) and CoPd nanoplates (Fig. 2h). It is obvious that the surface of the A4 paper is fully coated by a layer of pencil graphite (Fig. 2a and b). The graphite layer tightly adheres to the paper surface, which provides a good electric conductivity and forms a transition layer for the electrodeposition of Co nano-plates. Besides, the preparation of the conductive PG substrate does not employ any binder, which ensures a high stability in the long time test. And there is no loss of the active materials falling off from the PG substrate during the electrochemical reaction. At low magnification, the Co and CoPd uniformly distribute on the surface of the PG substrate and forms a Co and CoPd film (Fig. 2c and e). At high magnification, it is obvious that the Co film is comprised by many Co nano-plates and the diameter of the Co nanoplates is around 500 nm (Fig. 2d). All of the nano-plates are crisscross and exhibit a 3D nano structure, which is favorable for the diffusion of fuel during the electrochemical reaction and may lead a high catalytic performance. In addition, the existence of the metallic Co film improves the electronic conductivity of the PG substrate, which is benefit for the transfer of electrons. After the attachment of the Pd

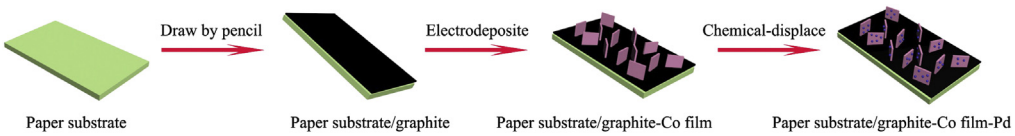

Fig. 1. Fabrication process of paper substrate/graphite-Co film-Pd electrode (PG-CoPd).

by the chemical-reduction method, the surface of the Co nano-plates become much rougher and are decorated with metallic Pd (Fig. 2f). Fig. 2g and h are the TEM images of the Co and CoPd nano-plates. The edges of the nano-plates are zigzag rather than straight, which will remarkably increase the surface area of the electrodes [26]. Compared with the sleek surface of the Co nano-plates (Fig. 2g), the surfaces of the CoPd nano-plates are coarser, which can be due to the attachment of the metallic Pd nanoparticles (Fig. 2h).

Fig. 3 shows the SEM image of PG-CoPd electrode (a), the corresponding elemental distributions of C (Fig. 3b), Co (Fig. 3c) and Pd (Fig. 3d). It is obvious that the Co forms a film-like metallic layer at low magnification in the surface of graphite layer (Fig. 3a). Apparently, the C element distributes is unfocused (Fig. 3b), which suggests that the Co film does not completely cover the graphite and some gaps exist among the Co film and it is consistent with Fig. 2c. Fig. 3c and d demonstrate that the Co and Pd elements uniformly distribute in the surface of graphite layer.

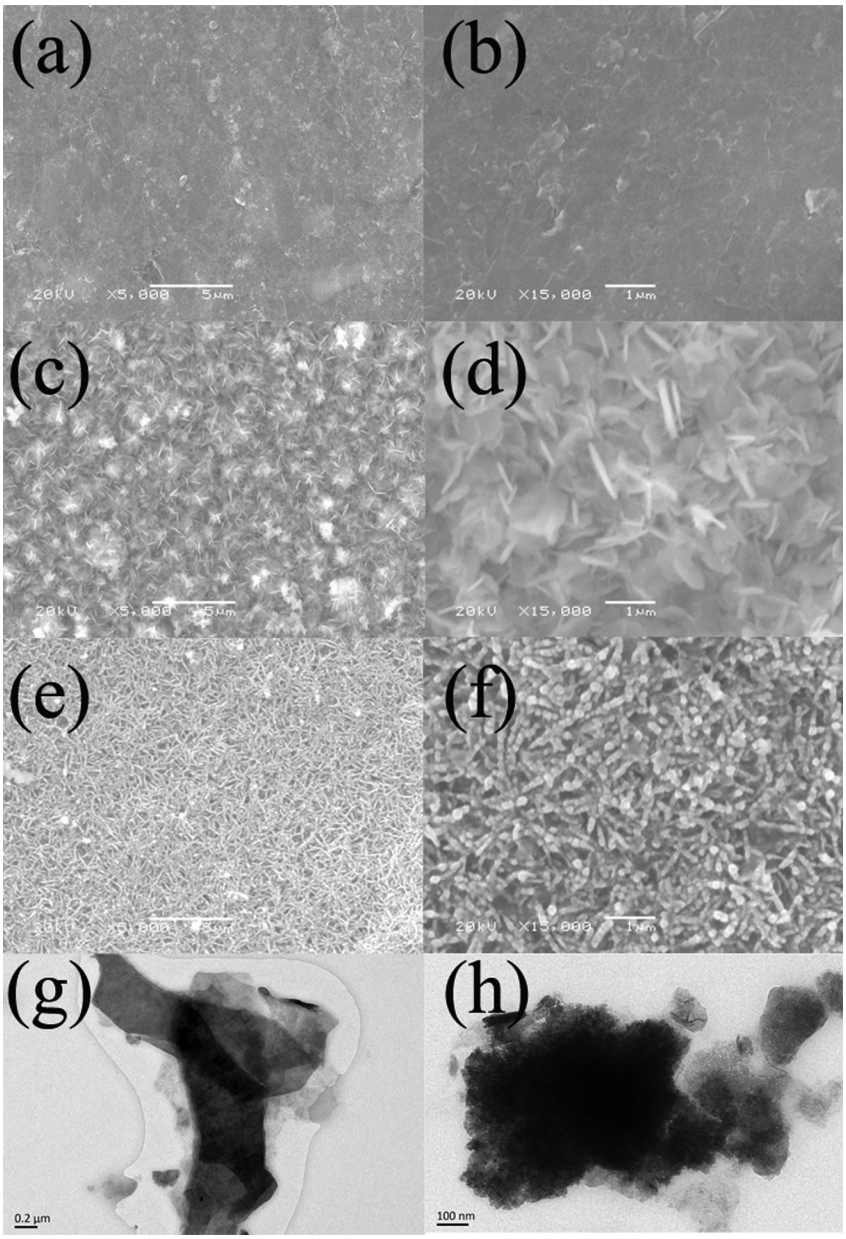

Fig. 2. SEM images of PG (a and b), PG-Co (c and d), PG-CoPd electrode (e and f) and TEM images of the Co (g) and CoPd nanoplates (h).

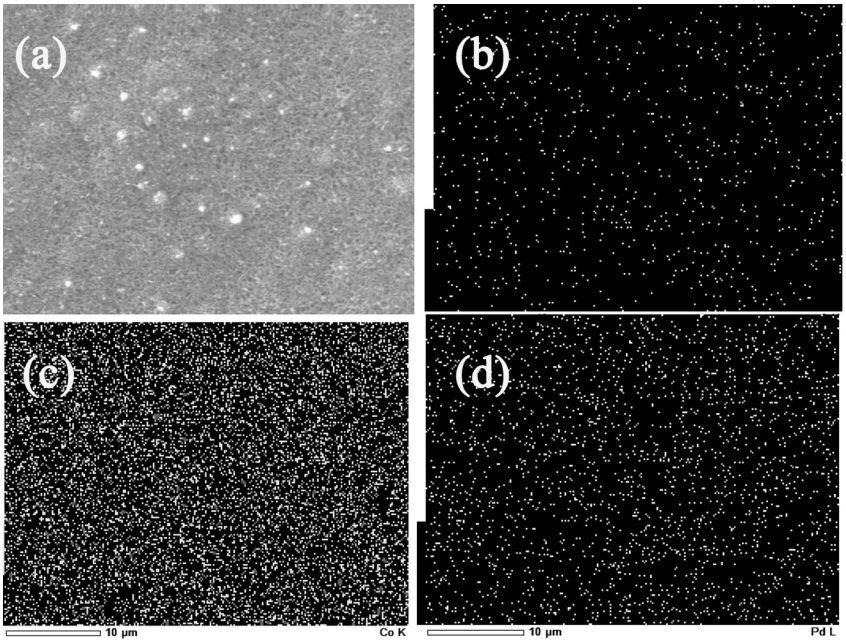

Fig. 3. SEM image of PG-CoPd electrode (a), the corresponding elemental distributions of C (b), Co (c) and Pd (d).

The XRD patterns of the PG, PG-Co and PG-CoPd are shown in Fig. 4. It is obvious that the PG substrate exhibits some diffraction peaks between 15° and 60°, which can be attributed to the carbon contained calcium salt (The main ingredient of the A4 paper and pencil lead, Eg. Cellulose, hemicellulose, lignin, $CaCO_3$, $CaSO_4$). Compared with the bare PG substrate, the PG-Co electrode displays five well-defined diffraction peaks at 2θ values of 48.8°, 52.1°, 55.9°, 60.5°, 73.1°. All of these peaks can be successfully indexed to (1 0 0), (0 0 2), (1 0 1), (2 0 0) and (1 1 0) plane reflections of the metallic Co (JCPDS Card NO. 05-0727). After doping Pd, two characteristic peaks of Pd at 48.2° and 81.8° matched well with the (1 1 1) and (3 1 1) plane reflections of Pd, according to the standard crystallographic spectrum of Pd (JCPDS card No. 65-2867). The diffraction peaks of Pd is obviously much weaker than that of Co suggesting that a small amount of Pd was deposited on the Co nano-plates [18].

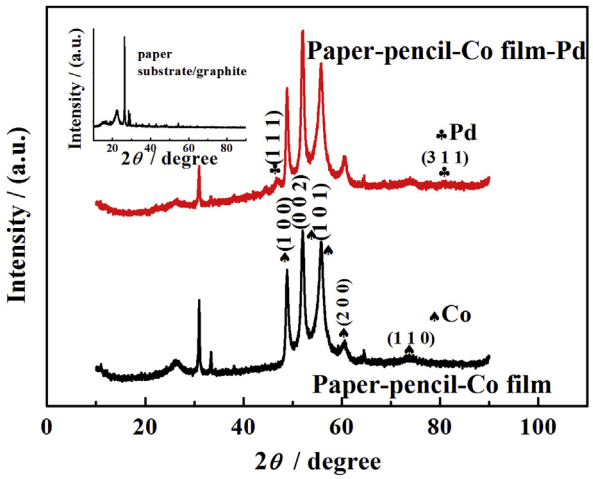

Fig. 4. XRD patterns of the PG, PG-Co and PG-CoPd.

Cyclic voltammograms (CVs) of PG-Co and PG-CoPd electrodes in 0.5 mol dm^{-3} NaOH solution at a scan rate of 50 mV s^{-1} are shown in Fig. 5a. The CV of PG-Co exhibits redox peaks at around −0.7 V and +0.2 V, which can be attributed to the redox couple of Co itself [20,33–35]. Compared with the pure Co electrode, the CoPd exhibits a strong anodic peak at around −0.7 V and an obvious cathodic peak appears at around −0.4 V, which can be ascribed to the electrooxidation of hydrogen releasing from the hydrogen evolution reaction and the electroreduction of Pd surface oxides [20]. Besides, it is obvious that the redox current density using CoPd is higher than the using of pure Co electrode, which suggests that the CoPd has a larger electrochemically active surface area (EASA) than the Co. Fig. 5b shows the CVs of PG-Co and PG-CoPd electrodes in 1 mol dm^{-3} NaOH and 0.6 mol dm^{-3} H_2O_2 at a scan rate of 10 mV s^{-1}. As can be seen, the electroreduction current density is only about −42 mA cm^{-2} at −0.35 V on PG-Co. However, the CV exhibits a H_2O_2 reduction peak on the same potential and the electroreduction current density reaches to −130 mA cm^{-2} on PG-CoPd, which is almost three times of that of the PG-Co. The result may be caused by three factors: first, the precious metal has a higher catalytic activity than transition metals or their oxides; second, the PG-CoPd has a higher EASA than PG-Co (Fig. 5a); third, the metallic Co may be partly oxidized to oxidation state in strong oxidizing solution (NaOH and H_2O_2) and the electronic conductivity may decrease during the reaction process and the existence of Pd improves the conductivity [20].

Fig. 6 shows the effect of H_2O_2 concentration on the catalytic performance of the PG-CoPd electrode for H_2O_2 electroreduction in 1 mol dm^{-3} NaOH. As seen from the CVs, all of the open circuit potentials (OCP) on PG-CoPd are around −0.15 V, suggesting that the OCP is independent with the H_2O_2 concentration. At low H_2O_2 concentration (0.2–0.8 mol dm^{-3}), there is an obvious H_2O_2 reduction peak among −0.18 to −0.48 V and the reduction peak moves to more negative with the increase of the H_2O_2 concentration. However, the reduction peaks disappear when the H_2O_2 concentrations increased to 1.0 and 1.4 mol dm^{-3}. Besides, with the increase of H_2O_2 concentration from 0.2 to 1.4 mol dm^{-3}, the electroreduction current density increased remarkably from −22

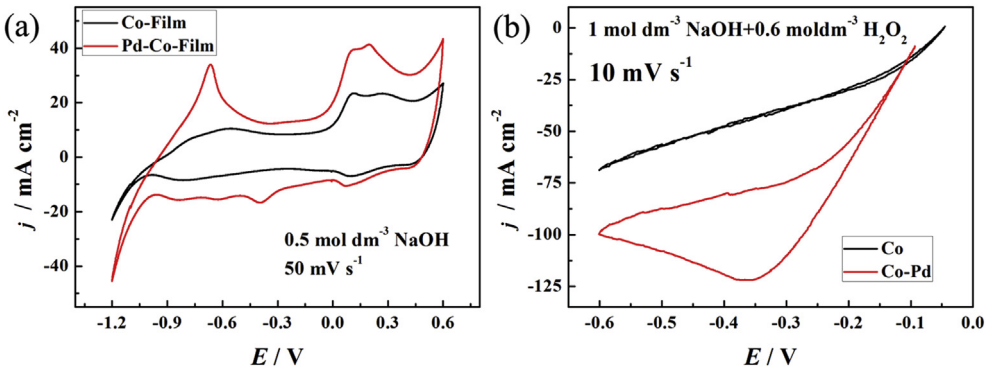

Fig. 5. Cyclic voltammograms (CVs) of PG-Co and PG-CoPd electrodes in 0.5 mol dm^{-3} NaOH solution at a scan rate of 50 mV s^{-1} (a); CVs of PG-Co and PG-CoPd electrodes in 1 mol dm^{-3} NaOH and 0.6 mol dm^{-3} H_2O_2 at a scan rate of 10 mV s^{-1} (b).

to −270 mA cm^{-2} at −0.6 V. The mount of the H_2O_2 that diffused to the surface of the PG-CoPd increases with increasing the H_2O_2 concentration, which will lead to a higher performance. To directly explain the efficiency of Pd on the PG-Co electrode, the current density unit was expressed as A cm^{-2} mg^{-1}. The Pd loading in the PG-CoPd electrode is about 0.0535 mg cm^{-2} and the electroreduction current density reaches to −4.30 A cm^{-2} mg^{-1} in 1 mol dm^{-3} NaOH and 1.4 mol dm^{-3} H_2O_2 at −0.5 V, which is much higher than the Au/Pd doped Ni foam electrodes [18]. The superior electrocatalyst for H_2O_2 electroreduction may be ascribed to the especial 3D nano structure and the high specific area. Besides, the performance of as-prepared PG-CoPd electrode is higher than the Pd modified porous Co electrode (−4.00 A cm^{-2} mg^{-1} at −0.5 V in 1.5 mol dm^{-3} H_2O_2) and more than two times than the Au modified porous Co electrode for H_2O_2 electroreduction (−2.10 A cm^{-2} mg^{-1} at −0.5 V in 1.5 mol dm^{-3} H_2O_2) [18]. However, the deformability, light weight and degradability of the A4 paper are much more predominant than the normal metal substrate.

In order to investigate the stability of the electrode, H_2O_2 electroreduction at various constant potentials was performed. The chronoamperometric curves (CAs) are shown in Fig. 7. The reduction current densities steady at −58, −100, −148 and −167 mA cm^{-2} after 7200 s, respectively, when the potentials are fixed at −0.2, −0.3, −0.4 and −0.6 V. When increase the cathode potential, the electroreduction reaction obtains a high driving force and is more favorable for the reaction process [17,20,33]. The CAs stable after 100 s and keep a high stability during the whole test process, which may be attributed to the unfallen electrode catalysts and stable electrode structure.

The reaction temperature has great influence on the electrochemical behavior of H_2O_2 electroreduction. Fig. 8a shows the CVs of H_2O_2 electroreduction on the PG-CoPd in the solution containing 1 mol dm^{-3} NaOH and 0.6 mol dm^{-3} H_2O_2 at different temperatures. The performance of H_2O_2 electroreduction improved remarkably by increasing the reaction temperature. When the temperature increased from 294.15 to 355.15 K, the oxidation current density at −0.6 V increased from −100 to −480 mA cm^{-2}, which demonstrates that the higher temperature usually results in faster electrode kinetics as the previous report [36]. Besides, more H_2O_2 will diffuse to the surface of the PG-CoPd that causes the negative shift of the electroreduction peaks with the increase of temperatures. However, high temperature also results in high rate of H_2O_2 hydrolysis, which could reduce the utilization of H_2O_2. Therefore, operating at low temperature is important for minimizing gas evolution and achieving high utilization of the oxidizer. The activation energy for the electrooxidation of H_2O_2 on PG-CoPd electrode was calculated to be 8.466 kJ mol^{-1} obtained from the Arrhenius relationship (Eq. (2)) [37]. Where j is the current density; T is the thermodynamic temperature; R is the molar gas constant; and Ea is the activation energy. The logarithm of peak current densities (ln j) at −0.3 V were plotted against the reciprocal of absolute temperatures (T^{-1}) (Fig. 8b).

$$\frac{\partial \ln j}{\partial T} = -\frac{E_a}{RT^2} \quad (2)$$

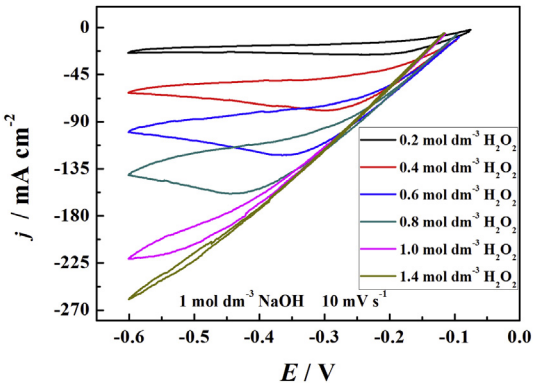

Fig. 6. CVs of PG-CoPd in 1 mol dm^{-3} NaOH and x mol dm^{-3} H_2O_2 (x = 0.2, 0.4, 0.6, 0.8, 1.0 and 1.4) at a scan rate of 10 mV s^{-1}.

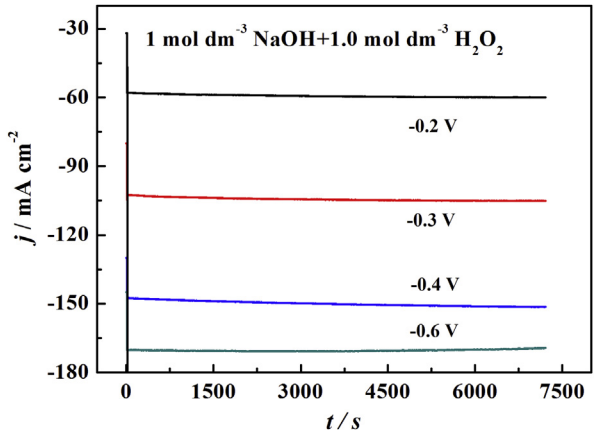

Fig. 7. Chronoamperometric curves (CAs) for H_2O_2 electroreduction at different potentials (−0.2, −0.4, −0.6 and −0.8 V) in 1 mol dm^{-3} NaOH and 1.0 mol dm^{-3} H_2O_2.

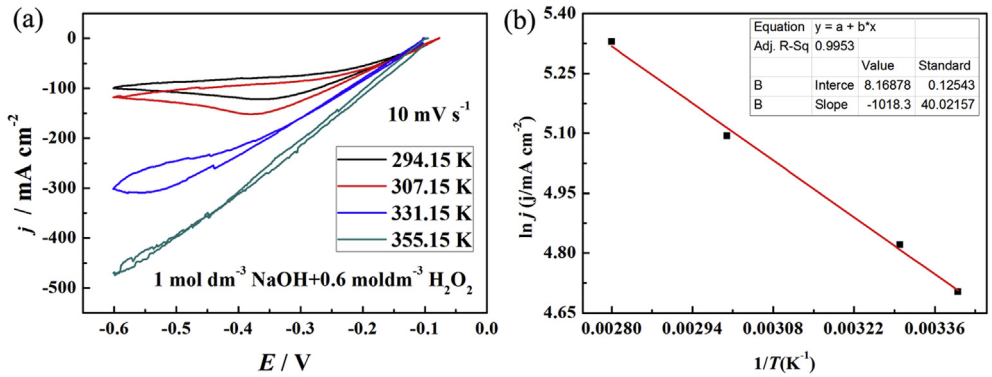

Fig. 8. CVs of H_2O_2 electroreduction on the PG-CoPd electrode in 1 mol dm^{-3} NaOH and 0.6 mol dm^{-3} H_2O_2 at different temperatures, Scan rate: 10 mV s^{-1} (a); Arrhenius plot of the current densities at −0.3 V for H_2O_2 electroreduction on the PG-CoPd electrode (b).

4. Conclusions

A high performance of PG-CoPd electrode with a 3D nano structure was successfully prepared via a facile method by simply coating a graphite layer on the surface of a normal A4 paper followed by Co electrodeposition and Pd chemical-reduction. The preparation process of the electrode does not employ any binder and the electrode exhibits high electrocatalytic performance and superior stability for H_2O_2 electroreduction in a NaOH solution. The simple fabrication, binder-free, light weight, high stability and environmentally friendly make the electrode a promising cathode of FCs.

Acknowledgments

We gratefully acknowledge the finance supported by the Fundamental Research Funds for the Central Universities (HEUCF201403018), the Heilongjiang Postdoctoral Fund (LBH-Z13059), the China Postdoctoral Science Foundation (2014M561332), and the National Natural Science Foundation of China (21403044).

Appendix A. Supplementary data

Supplementary data related to this article can be found at http://dx.doi.org/10.1016/j.jpowsour.2014.10.014.

References

[1] Ø. Hasvold, K.H. Johansen, O. Mollestad, S. Forseth, N. Størkersen, J. Power Sources 80 (1999) 254–260.
[2] R.R. Bessette, M.G. Medeiros, C.J. Patrissi, C.M. Deschenes, C.N. LaFratta, J. Power Sources 96 (2001) 240–244.
[3] E.G. Dow, R.R. Bessette, G.L. Seeback, C. Marsh-Orndorff, H. Meunier, J. VanZee, M.G. Medeiros, J. Power Sources 65 (1997) 207–212.
[4] G.H. Miley, N. Luo, J. Mather, R. Burton, G. Hawkins, L. Gu, E. Byrd, R. Gimlin, P.J. Shrestha, G. Benavides, J. Laystrom, D. Carroll, J. Power Sources 165 (2007) 509–516.
[5] D.M.F. Santos, P.G. Saturnino, R.F.M. Lobo, C.A.C. Sequeira, J. Power Sources 208 (2012) 131–137.
[6] L. Yi, L. Liu, X. Liu, X. Wang, W. Yi, P. He, X. Wang, Int. J. Hydrogenen Energy 37 (2012) 12650–12658.
[7] W. Sung, J.-W. Choi, J. Power Sources 172 (2007) 198–208.
[8] J. Zhu, R.R. Sattler, A. Garsuch, O. Yepez, P.G. Pickup, Electrochim. Acta 51 (2006) 4052–4060.
[9] J.R.C. Salgado, J.C.S. Fernandes, A.M. Botelho do Rego, A.M. Ferraria, R.G. Duarte, M.G.S. Ferreira, Electrochim. Acta 56 (2011) 8509–8518.
[10] S.-i. Yamazaki, Z. Siroma, H. Senoh, T. Ioroi, N. Fujiwara, K. Yasuda, J. Power Sources 178 (2008) 20–25.
[11] A.E. Sanli, A. Aytaç, Int. J. Hydrogenen Energy 36 (2011) 869–875.
[12] F. Yang, K. Cheng, Y. Mo, L. Yu, J. Yin, G. Wang, D. Cao, J. Power Sources 217 (2012) 562–568.
[13] F. Yang, K. Cheng, X. Liu, S. Chang, J. Yin, C. Du, L. Du, G. Wang, D. Cao, J. Power Sources 217 (2012) 569–573.
[14] F. Yang, K. Cheng, X. Xue, J. Yin, G. Wang, D. Cao, Electrochim. Acta 107 (2013) 194–199.
[15] L. Deng, M. Zhou, C. Liu, L. Liu, C. Liu, S. Dong, Talanta 81 (2010) 444–448.
[16] M.S. Tunuli, Talanta 39 (1992) 85–90.
[17] K. Cheng, F. Yang, D. Zhang, J. Yin, D. Cao, G. Wang, Electrochim. Acta 105 (2013) 115–120.
[18] F. Yang, K. Cheng, K. Ye, X. Xiao, F. Guo, G. Wang, D. Cao, J. Power Sources 257 (2014) 156–162.
[19] X. Qin, H. Wang, X. Wang, Z. Miao, Y. Fang, Q. Chen, X. Shao, Electrochim. Acta 56 (2011) 3170–3174.
[20] K. Cheng, F. Yang, Y. Xu, L. Cheng, Y. Bao, D. Cao, G. Wang, J. Power Sources 240 (2013) 442–447.
[21] L. Zhang, Y. Ni, X. Wang, G. Zhao, Talanta 82 (2010) 196–201.
[22] R.X. Feng, H. Dong, Y.D. Wang, X.P. Ai, Y.L. Cao, H.X. Yang, Electrochem. Commun. 7 (2005) 449–452.
[23] X. Xie, M. Pasta, L. Hu, Y. Yang, J. McDonough, J. Cha, C.S. Criddle, Y. Cui, Energy Environ. Sci. 4 (2011) 1293–1297.
[24] G. Yu, L. Hu, M. Vosgueritchian, H. Wang, X. Xie, J.R. McDonough, X. Cui, Y. Cui, Z. Bao, Nano Lett. 11 (2011) 2905–2911.
[25] W. Chen, R.B. Rakhi, L. Hu, X. Xie, Y. Cui, H.N. Alshareef, Nano Lett. 11 (2011) 5165–5172.
[26] D. Zhang, K. Cheng, N. Shi, F. Guo, G. Wang, D. Cao, Electrochem. Commun. 35 (2013) 128–130.
[27] D. Zhang, K. Ye, K. Cheng, Y. Xu, J. Yin, D. Cao, G. Wang, RSC Adv. 4 (2014) 17454–17460.
[28] T.H. Nguyen, A. Fraiwan, S. Choi, Biosens. Bioelectron. 54 (2014) 640–649.
[29] L. Hu, J.W. Choi, Y. Yang, S. Jeong, F. La Mantia, L.-F. Cui, Y. Cui, Proc. Nat. Acad. Sci. U. S. A. 106 (2009) 21490–21494.
[30] Q. Cheng, Z. Song, T. Ma, B.B. Smith, R. Tang, H. Yu, H. Jiang, C.K. Chan, Nano Lett. 13 (2013) 4969–4974.
[31] L. Nyholm, G. Nyström, A. Mihranyan, M. Strømme, Adv. Mater. 23 (2011) 3751–3769.
[32] D.-H. Kim, Y.-S. Kim, J. Wu, Z. Liu, J. Song, H.-S. Kim, Y.Y. Huang, K.-C. Hwang, J.A. Rogers, Adv. Mater. 21 (2009) 3703–3707.
[33] G. Wang, D. Cao, C. Yin, Y. Gao, J. Yin, L. Cheng, Chem. Mater. 21 (2009) 5112–5118.
[34] J. Liu, R. Liu, C.L. Yuan, X.P. Wei, J.L. Yin, G.L. Wang, D.X. Cao, Fuel Cells 13 (2013) 903–909.
[35] H.-B. Noh, K.-S. Lee, P. Chandra, M.-S. Won, Y.-B. Shim, Electrochim. Acta 61 (2012) 36–43.
[36] K. Cheng, D. Cao, F. Yang, D. Zhang, P. Yan, J. Yin, G. Wang, J. Power Sources 242 (2013) 141–147.
[37] D. Cao, L. Sun, G. Wang, Y. Lv, M. Zhang, J. Electroanal. Chem. 621 (2008) 31–37.